Supplemental Document

Optics EXPRESS

Unsupervised hyperspectral stimulated Raman microscopy image enhancement: denoising and segmentation via one-shot deep learning: supplement

PEDRAM ABDOLGHADER,[1,2] ANDREW RIDSDALE,[2] TASSOS GRAMMATIKOPOULOS,[3] GAVIN RESCH,[1] FRANÇOIS LÉGARÉ,[4] ALBERT STOLOW,[1,2,5,6,7] ADRIAN F. PEGORARO,[1,2,9] AND ISAAC TAMBLYN[1,8,10]

[1]*Department of Physics, University of Ottawa, Ottawa, ON, K1N 6N5, Canada*
[2]*Security and Disruptive Technologies, National Research Council Canada, Ottawa, ON, K1A 0R6, Canada*
[3]*SGS Canada Inc, Lakefield, ON, Canada*
[4]*Institut National de la Recherche Scientifique, Centre EMT, Varennes, QC, J3X1S2, Canada*
[5]*NRC-uOttawa Joint Centre for Extreme Photonics, Ottawa ON K1N 6N5, Canada*
[6]*Max-Planck-uOttawa Centre for Extreme and Quantum Photonics, Ottawa ON K1N 6N5, Canada*
[7]*Department of Chemistry, University of Ottawa, Ottawa, ON, K1N 6N5, Canada*
[8]*Vector Institute for Artificial Intelligence, Toronto, Ontario, Canada*
[9]*apegorar@uottawa.ca*
[10]*isaac.tamblyn@uottawa.ca*

Supplement DOI: https://doi.org/10.6084/m9.figshare.16705603

Parent Article DOI: https://doi.org/10.1364/OE.439662

Unsupervised Hyperspectral Image Enhancement, Segmentation and De-Noising in Stimulated Raman Microscopy: supplemental document

1. First model

A 10-layer convolutional autoencoder trained in order to denoise the hyperspectral SRS microscopy images. Convolutional layers in the encoder modules compressed the dataset dimension and mapped them to the latent space. The latent space can be considered a feature vector where applying deconvolutional layers (CovT) on it leads to reconstructing the input dataset. Figure S1 demonstrates the first model architecture and its parameters. The dataset that was fed into this model was spectra from a mixture of hexadecane and water. Input dataset shape was 65536 signals each with a length of 92 points and one channel.

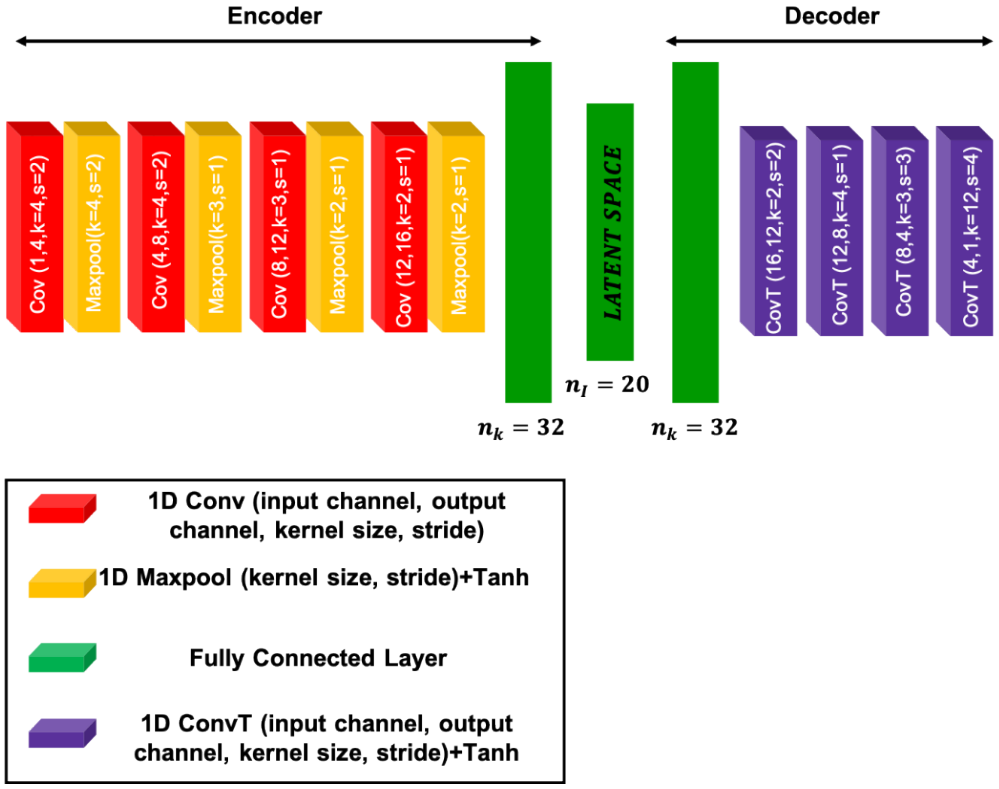

Fig. S.1. First model architecture and its parameters.

2. Second model

Figure S2 demonstrates the second model architecture and its parameters. The dataset fed into this model was spectra from a mixture of mineral ores. Input dataset shape was 65536 signals each with a length of 909 points and one channel.

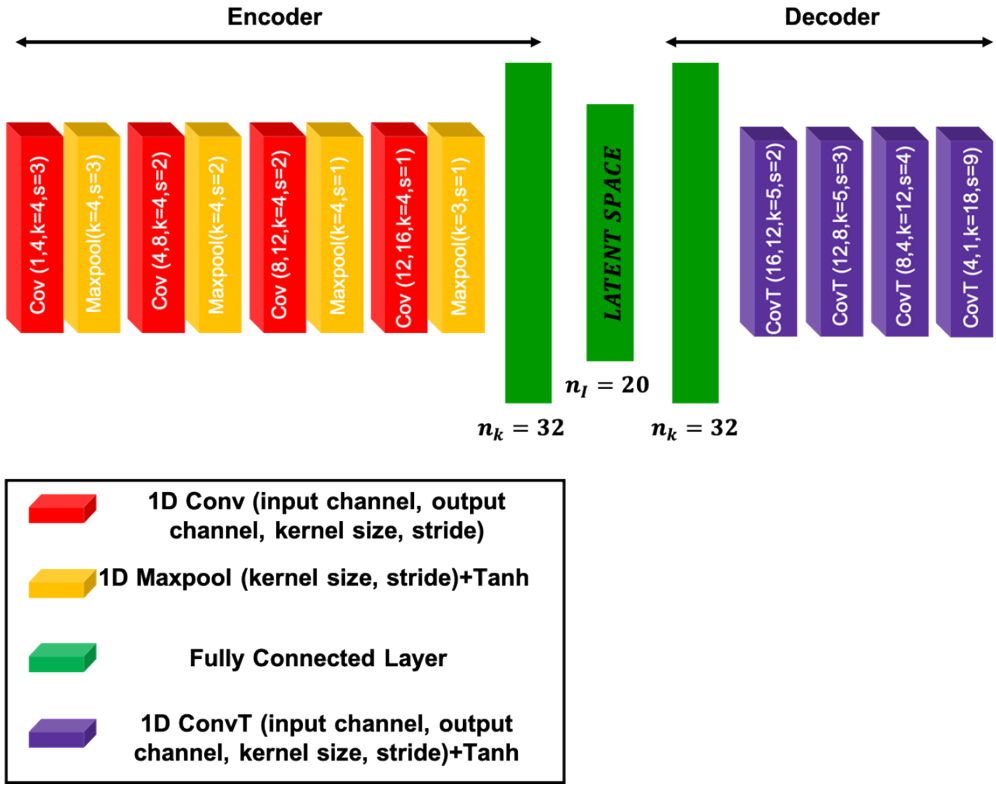

Fig. S2. Second model architecture and its parameters.

3. Elbow method in order to determine the best number of clusters in the latent space

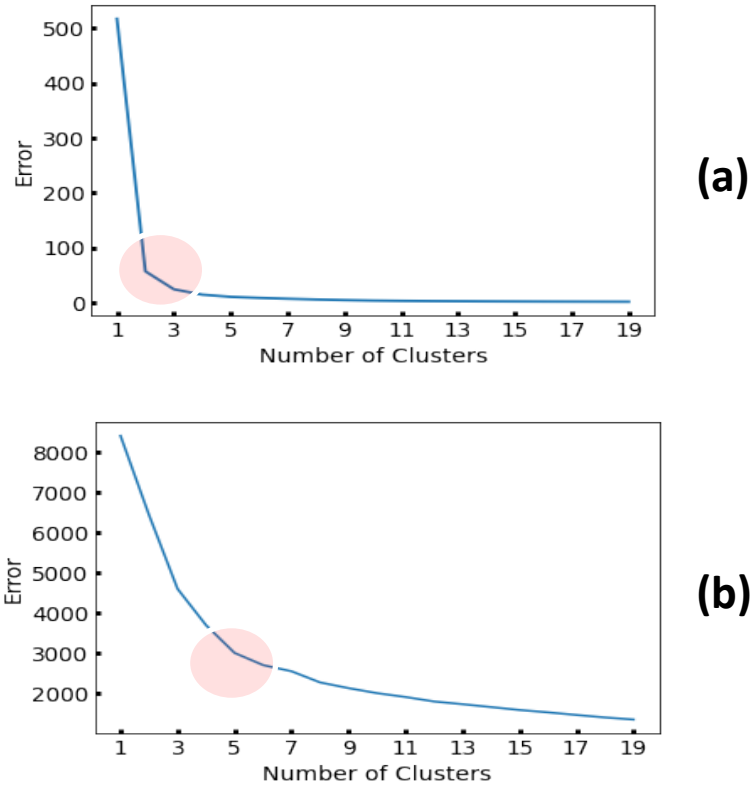

Fig. S3. Applying elbow method on the latent space (with *k*-mean algorithm) to determine the best number of clusters in latent space. (a): On hexadecane and water sample, (b) on mineral ore sample.

4. Spatial distribution of error showing the effect of a moving boundary between the ground truth and the noisy input image

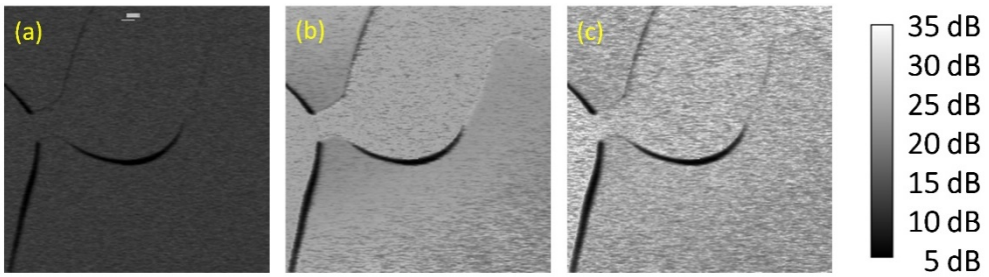

Fig. S4. The spatial distribution of the PSNR for FOV1 for the data presented in Fig. 5 for (a) Input-GT, (b) SHRED-GT, and (c) UHRED-GT. It is apparent that there was a shift in the boundary between the hexadecane and water phases which affects all comparisons equally.

Data Availability. All data used in this study is available at Ref. [1]. All algorithms and source code are available at Ref. [2].

References

[1] P. Abdolghader, "Unsupervised hyperspectral stimulated Raman microscopy image enhancement: De-noising and segmentation via one-shot deep learning," 2021, http://clean.energyscience.ca/datasets/
[2] P. Abdolghader, "Unsupervised and supervised deep neural network models working with stimulated Raman spectroscopy microscopes", (2021) http://clean.energyscience.ca/codes